Int. J. Heat Mass Transfer. Vol. 36, No. 9, pp. 2317–2326, 1993
Printed in Great Britain

0017-9310/93 $6.00 + 0.00
Pergamon Press Ltd

A two-port network formalism for 3D heat conduction analysis in multilayered media

PH. LETURCQ, J. M. DORKEL, F. E. RATOLOJANAHARY and S. TOUNSI

Laboratoire d'Automatique et d'Analyse des Systèmes du CNRS, 7 Avenue du Colonel Roche, 31077 Toulouse Cedex, France

Institut National des Sciences Appliquées de Toulouse, Complexe Universitaire de Rangueil, 31077 Toulouse Cedex, France

(*Received* 19 *March* 1992 *and in final form* 19 *October* 1992)

Abstract—This paper demonstrates that the two-port network formalism, commonly used to treat one-dimensional heat flow problems in composite slabs, is also applicable to three-dimensional problems in the context of integral transform methods. This provides easy calculation means for temperature and heat flux distributions within multilayered systems. Both spectral and superposition methods are thus presented as examples in a variety of cases of interest to engineers.

1. INTRODUCTION

CONDUCTIVE heat transfer through multilayered media is a relevant problem in many engineering fields. For example, in power electronics the heat sinking of semiconductor devices mainly relies on the 3D heat conducting properties of the packaging materials.

At present, heat flow calculations in multilayered systems are successfully handled by purely numerical methods. Nevertheless, as far as the device geometry, boundary conditions and material properties (especially linearity) allow it, analytical approaches remain of interest to designers since they give a more synthetic insight into the influence of each parameter and generally lead to substantial computational savings.

The essentials of analytical approaches together with the major applications to the multilayer problem can be found in classical textbooks concerned with heat conduction [1, 2] or electrostatics [3]. Schematically, the various methods are based on variable separation in the heat equation, Green's functions and superposition principle, or integral transforms, and are closely related through the assumed linearity of the heat flow.

The published results, whatever method is used, are restricted to special cases involving a limited number of layers, featuring various geometrical shapes and boundary conditions. A typical example of this is a two or three-layer parallelepiped with heaters distributed at the top surface, adiabatic lateral faces and an isothermal bottom surface [4–6]. Also, the 3D-electrostatic potential Green's function has been derived for a three-layer medium of infinite lateral extent bounded by ground planes [7]. To our knowledge, no calculation procedure has been proposed for an unlimited number of layers except for Brook and Smith's analysis of the spreading resistance of axisymmetric multilayer cylinders [8, 9]. Indeed, besides cumbersome mathematical developments, the major difficulty in performing analytical solutions to the multiple-layer problem arises from the boundary conditions that couple adjacent layers.

This paper proposes a method for circumventing this difficulty. It introduces a two-port matrix formalism in the 3D analysis of heat flow through multilayered media. The two-port formalism derived from the circuit theory is already known in the field of heat conduction where it has been applied to one-dimensional transient problems through composite slabs [1, 10–12]. Here, the aim is to show that this formalism is also applicable to three-dimensional problems. This will allow the previous analysis to be generalized, and will provide easy means of calculation for temperature and heat flux distributions in multilayered systems, in the context of integral transform methods. In addition, it will be shown that the two-port matrix formalism gives a theoretical basis for thermal characterization of multilayered devices.

2. DEFINITION OF THE PROBLEM

The structure of interest is shown in Fig. 1. It consists of adjacent material layers labelled $\ldots i, i+1 \ldots$ with plane parallel boundaries between them. Each layer of width w_i is assumed to be homogeneous and isotropic with constant thermal conductivity k_i and diffusivity D_i. The interfaces are not necessarily ideal and a contact conductance g_i per unit area will be considered between each layer i and the following one.

The lateral extent of the system may be infinite or

NOMENCLATURE

a	radius of a circular heat source
$[A_i]$	characteristic chain-matrix relative to layer i
$A_{11}, A_{12}, A_{21}, A_{22}$	chain-matrix parameters
c	thermal influence function
D_i	thermal diffusivity of the i-layer material
g_i	contact conductance between the i- and $i+1$-layer
H_{11}	hybrid-matrix parameter
J_0, J_1	Bessel functions of the first kind of order zero and one respectively
k_i	thermal conductivity of the i-layer material
L, l	length and width of a rectangular contour
m, m^*	wave number or spatial angular frequency
p	density of dissipated power
P	total dissipated power
R_{th}	thermal resistance
s	complex angular frequency
t	time variable
w_i	thickness of layer i
x, y, z	Cartesian coordinates
z_1, z_2, z_i	ordinates of plane boundaries
$Z_{11}, Z_{12}, Z_{21}, Z_{22}$	impedance-matrix parameters.

Greek symbols

Φ_i	z-component of the transformed heat flux density in layer i
ρ	radial distance
θ_i	temperature rise in layer i
Θ_i	transform of the temperature rise in layer i
ξ, η	spatial coordinates.

finite. In the latter case, the variety of geometrical shapes (e.g. parallelepipedic, circular cylinder, ...) and boundary conditions (e.g. adiabatic, isothermal, ...) which can be considered is inevitably restricted by the availability of adequate transformations. This will be discussed in Section 4.

Heat sinking and arbitrary heat sources are assumed to be provided at the opposite limiting planes of the system, no heat being generated in the bulk layers.

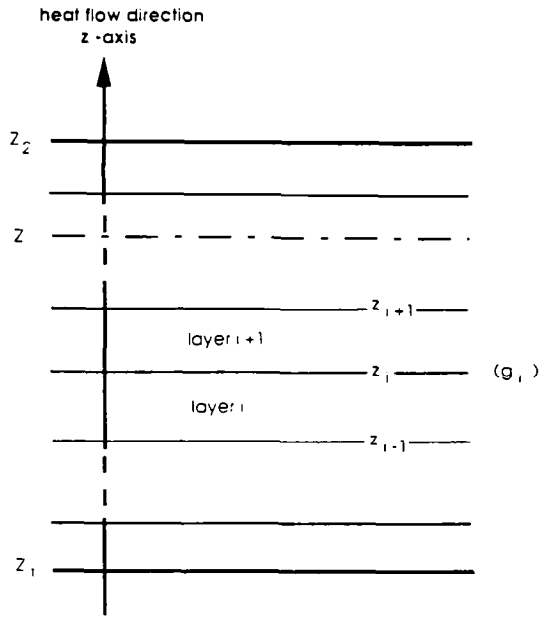

FIG. 1. Schematic representation of the multilayer system and symbols used in theoretical analysis.

Thus, the temperature increase $\theta_i(\xi, \eta, z, t)$ in each layer i is the solution of the 3D heat conduction equation:

$$\nabla^2\theta_i = \frac{1}{D_i}\frac{\delta\theta_i}{\delta t} \tag{1}$$

subject to the appropriate boundary conditions. The coordinates (ξ, η, z) may be either cartesian (x, y, z) or cylindrical (ρ, θ, z), as the case may be.

3. GENERAL APPROACH

3.1. *Steady heat flow*

For clarity, first consider steady heat flow. Then, equation (1) reduces to Laplace's equation:

$$\nabla^2\theta_i(\xi, \eta, z) = 0. \tag{2}$$

It is well-known that the use of some double integral transformations in the coordinates ξ, η may reduce equation (2) to the following ordinary differential equation:

$$\frac{d^2\Theta_i}{dz^2} = m^2\Theta_i \tag{3}$$

where the transform Θ_i of the temperature θ_i depends on a new set of variables (μ, ν, z) and m is linked to μ and ν. However, this reduction only occurs if the transformation is compatible with the prescribed lateral boundary conditions, as discussed in Section 4. Examples of these linear operators are the double Fourier transform for laterally unlimited systems or the zero-order Hankel transform in case of axisymmetry, the double finite sine and cosine transforms in parallelepipedic systems with isothermal (sine) or adiabatic (cosine) lateral boundary conditions [13].

If the adequate transformation exists, the general solution for Θ_i is simply

$$\Theta_i = C_i e^{-mz} + C'_i e^{+mz} \quad (4)$$

where C_i and C'_i are functions of the transformed variables.

The transform Φ_i of the z-component $(-k_i \delta\theta_i/\delta z)$ of the heat flux distribution in the i-layer is obtained from this result

$$\Phi_i = mk_i C_i e^{-mz} - mk_i C'_i e^{+mz}. \quad (5)$$

At the boundary $z = z_i$ between the ith and $(i+1)$th layers, the continuity of the z-component of heat flux generally imposes a temperature jump

$$\theta_i(z_i^+) - \theta_i(z_i^-) = \frac{k_i}{g_i} \frac{\delta\theta_i}{\delta z}\bigg|_{z_i} \quad (6)$$

where g_i is the contact conductance between both layers, relative to the unit area.

Because of linearity, this condition still holds for temperature transforms

$$\Theta_i(z_i^+) - \Theta_i(z_i^-) = \frac{k_i}{g_i} \frac{d\Theta_i}{dz}\bigg|_{z_i}. \quad (7)$$

Therefore, it follows from equation (4) that

$$\Theta_i(z_i^+) = (1 - mk_i/g_i) C_i e^{-mz_i} + (1 + mk_i/g_i) C'_i e^{+mz_i}. \quad (8)$$

Now, consider the transforms of temperature and heat flux at the boundaries of the i-layer, including the non-ideal interface with the $(i+1)$th layer. Let

$$\begin{aligned}
\Theta_{i1} &= \Theta_i(z_{i-1}^+) = C_i e^{-mz_{i-1}} + C'_i e^{+mz_{i-1}} \\
\Theta_{i2} &= \Theta_i(z_i^+) = (1 - mk_i/g_i) C_i e^{-mz_i} + (1 + mk_i/g_i) C'_i e^{+mz_i} \\
\Phi_{i1} &= \Phi_i(z_{i-1}) = mk_i C_i e^{-mz_{i-1}} - mk_i C'_i e^{+mz_{i-1}} \\
\Phi_{i2} &= \Phi_i(z_i) = mk_i C_i e^{-mz_i} - mk_i C'_i e^{+mz_i}.
\end{aligned} \quad (9)$$

Eliminating the unknown functions C_i and C'_i leads to

$$\begin{aligned}
\Theta_{i1} &= \mathrm{ch}(mw_i)\Theta_{i2} + (\mathrm{sh}(mw_i)/(mk_i) + \mathrm{ch}(mw_i)/g_i)\Phi_{i2} \\
\Phi_{i1} &= mk_i \mathrm{sh}(mw_i)\Theta_{i2} + (m(k_i/g_i)\mathrm{sh}(mw_i) + \mathrm{ch}(mw_i))\Phi_{i2}
\end{aligned} \quad (10)$$

where w_i is the i-layer width, or, using a matrix notation

$$\begin{bmatrix} \Theta_{i1} \\ \Phi_{i1} \end{bmatrix} = [A_i(m)] \begin{bmatrix} \Theta_{i2} \\ \Phi_{i2} \end{bmatrix} \quad (11)$$

with

$$[A_i(m)] = \begin{bmatrix} \mathrm{ch}(mw_i) & \dfrac{\mathrm{sh}(mw_i)}{mk_i} + \dfrac{\mathrm{ch}(mw_i)}{g_i} \\ mk_i \mathrm{sh}(mw_i) & m(k_i/g_i)\mathrm{sh}(mw_i) + \mathrm{ch}(mw_i) \end{bmatrix}. \quad (12)$$

$[A_i(m)]$ is a chain-matrix (or transmission matrix) according to the four terminal (two-port) network theory. It connects the transforms of the 'input' and 'output' temperature and flux distributions relative to the i-layer. This implies an analogy between heat conduction through multilayered media and signal transmission through a cascade of two-port low-pass filters.

For a long time, this analogy has been recognized and used together with Fourier or Laplace transforms operating on the time variable t, in order to solve 1D problems, for instance in composite slabs [1, 10–12]. However, the formal identity between the matrix parameter expressions in (12) and those encountered in the study of unsteady 1D heat flow must not hide the fact that the problem here is not time-dependent but actually three-dimensional in space. To our knowledge, the application of the four terminal network theory to spatial aspects of heat conduction has not been explored to date.

It readily follows that the variable m (wave number) plays the role of a spatial angular frequency and

—Matrix $[A_i(m)]$ characterizes the properties of steady thermal conduction in the i-layer, independently of the actual lateral boundary conditions.

—The characteristic matrix $[A]$ for a slab of n layers may simply be obtained by successively multiplying the corresponding matrices $[A_i]$

$$[A] = [A_1][A_2] \ldots [A_n]. \quad (13)$$

—Other matrices of the four terminal classical theory or the scattering matrix (S-parameters) of the wave theory may be used. The impedance $[Z]$, admittance $[Y]$ and hybrid $[H]$ matrices may be of particular interest [14].

—The usual concepts and results of the two-port network theory can be transposed. For instance, the reciprocity properties of passive networks apply to heat transfer through multilayer media: the determinant of matrix $[A]$ is equal to 1, the $[Z]$ and $[Y]$ matrices being antisymmetrical.

3.2. *Unsteady heat flow*

In the case of unsteady heat flow with zero initial temperature throughout the structure, a simultaneous use of the Laplace transform operating on the time and the spatial transformation in ξ and η allow to reduce equation (1) to

$$\frac{d^2\Theta_i}{dz^2} = \left(m^2 + \frac{s}{D_i}\right)^{1/2} \Theta_i \quad (14)$$

where s is the complex angular frequency. This ordinary differential equation would also hold for non-zero steady initial conditions if temperature variations rather than real temperatures were considered.

Thus, the above considerations relative to steady heat flow still apply but the difference lies in that the variable m should be replaced with:

$$m^* = \left(m^2 + \frac{s}{D_i}\right)^{1/2} \tag{15}$$

and the conclusions in terms of usefulness of the two-port network theory remain unchanged.

4. CALCULATION OF TEMPERATURE AND FLUX DISTRIBUTIONS

4.1. *Steady heat flow*

For clarity, again we consider the steady heat flow.

As stated above, the chain matrix $[A]$ relative to a multilayered medium bounded by two parallel planes $z = z_1$ and $z = z_2$ (see Fig. 1) provides two linear relationships between the temperature and heat flux transforms (or spectra) Θ_1, Φ_1 at $z = z_1$ and Θ_2, Φ_2 at $z = z_2$

$$\Theta_1 = A_{11}(m)\Theta_2 + A_{12}(m)\Phi_2$$
$$\Phi_1 = A_{21}(m)\Theta_2 + A_{22}(m)\Phi_2. \tag{16}$$

Thus, as soon as two of these transforms are known according to the conditions imposed at z_1 and z_2, the two others readily follow. The transforms Θ_z, Φ_z at any intermediate plane z are then obtained by using one of the two $[A]$ matrices relative to the media comprised between z_1 and z on the one hand, and z and z_2 on the other.

Therefore, in practice, calculation only requires selecting the adequate transforms, if they exist, allowing the lateral boundary conditions to be expressed in the m-spectral domain and the results to be returned in the spatial domain.

Representative cases are

(a) Multilayered medium of laterally infinite extent; axisymmetrical sources and sinks.

The zero-order Hankel transform applies to this situation

$$\mathrm{F}(m) = \int_0^\infty \rho \mathrm{f}(\rho) J_0(m\rho)\, \mathrm{d}\rho \tag{17}$$

where ρ is the radial distance from the symmetry z-axis and J_0 the Bessel function of the first kind of order zero. The inverse transform is

$$\mathrm{f}(\rho) = \int_0^\infty m\mathrm{F}(m) J_0(m\rho)\, \mathrm{d}m. \tag{18}$$

By way of example, let us calculate the maximum temperature reached in the system of Fig. 2 which models cooling of a semiconductor chip through a composite substrate and a radiator. A uniform heat flux distribution is considered over a circular area of radius a at the top surface of the substrate and a constant convective transfer coefficient h to a cooling fluid is assumed at the bottom.

From the general formulation equation (16), the temperature transform at the top $z = z_1$ for $\Theta_2 = 0$ at the bottom, $z = z_2$ can be expressed as

$$\Theta_1(m) = \frac{A_{12}(m)}{A_{22}(m)} \Phi_1(m) \tag{19}$$

or, using the hybrid parameter notation

$$\Theta_1(m) = H_{11}(m)\Phi_1(m). \tag{20}$$

In this example, the Hankel transform Φ_1 of the input heat flux distribution at z_1 is

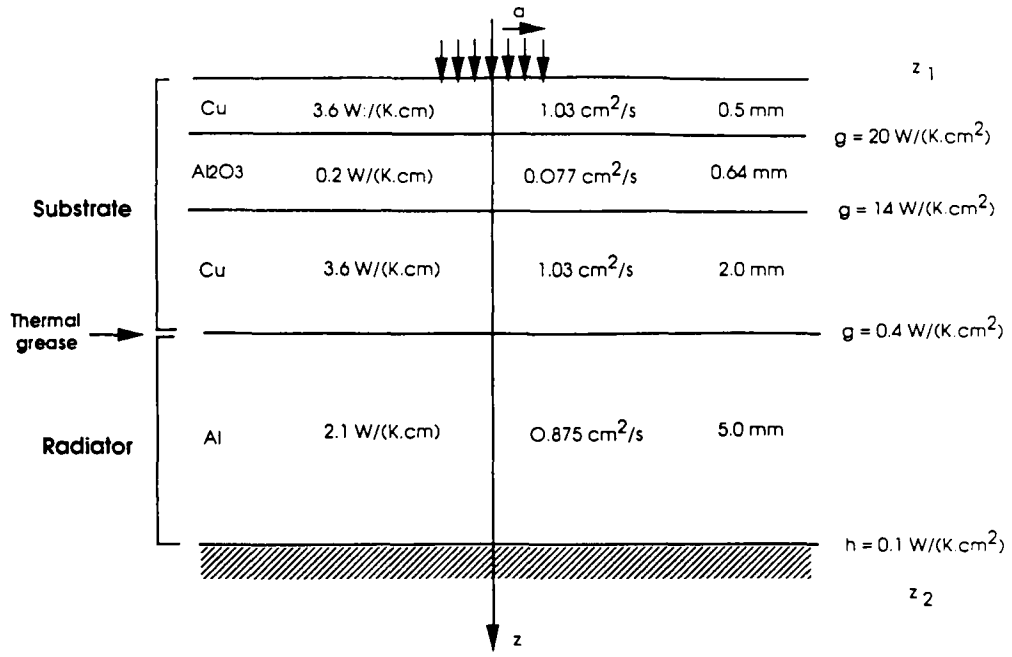

FIG. 2. Model for a power chip assembly and data (thermal conductivity, diffusivity, width) for calculations.

$$\Phi_1 = \frac{J_1(ma)}{\pi ma} P \tag{21}$$

where J_1 is the Bessel function of first order and P the injected power. The chain parameters A_{12} and A_{22} are obtained by multiplying the characteristic $[A]$ matrices, equation (12), of the successive layers from source to sink. For the bottom layer, the heat transfer coefficient h substitutes for the conductance g per unit area of the non-ideal interface. All operations up to equation (20) can be carried out explicitly but in practice are better performed numerically for a discrete set of values of m.

Then, the numerical computation of the inverse transform, equation (18) for $\Theta_1(m)$ (in practice reduced to the computation of a Bessel series) leads to the radial distribution $\theta(\rho)$ of the temperature rise at the top surface of the substrate. In particular, since the maximum temperature θ_{max} occurs at the origin $\rho = 0$, the apparent thermal resistance $R_{th} = \theta_{max}/P$ is given by

$$R_{th} = \int_0^\infty \frac{A_{12}(m)}{A_{22}(m)} \frac{J_1(ma)}{\pi a} \, dm. \tag{22}$$

The results are shown in Fig. 3 as a function of the radius a, for the substrate parameter values indicated in Fig. 2.

(b) Multilayered medium of infinite lateral extent; general case.

The double Fourier transformation applies. In Cartesian coordinates we have the following relations:

$$F(m_x, m_y) = \frac{1}{2\pi} \int_{-\infty}^{+\infty} \int_{-\infty}^{+\infty} f(x, y) e^{-j(m_x x + m_y y)} \, dx \, dy \tag{23}$$

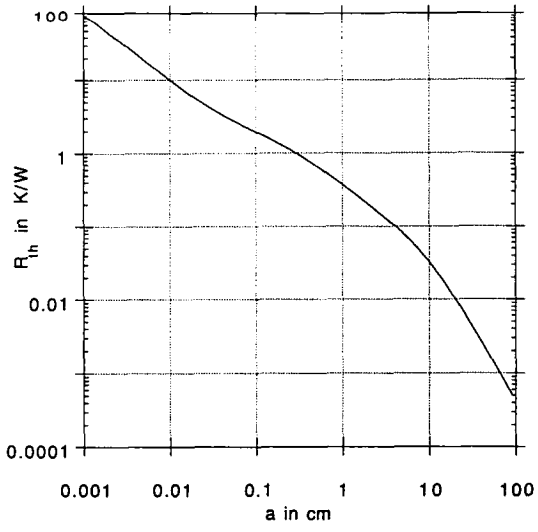

FIG. 3. Spreading thermal resistance of the system described in Fig. 2 as a function of the heat source radius.

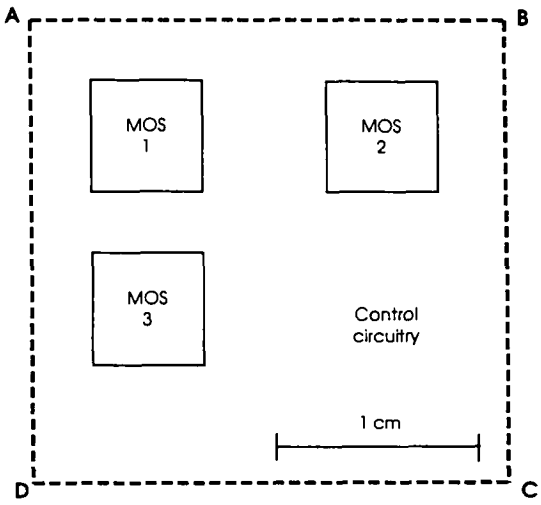

FIG. 4. Geometrical arrangement of a power MOS multichip module.

$$f(x, y) = \frac{1}{2\pi} \int_{-\infty}^{+\infty} \int_{-\infty}^{+\infty} F(m_x, m_y) \times e^{j(m_x x + m_y y)} \, dm_x \, dm_y. \tag{24}$$

In this case, the m variable of the $[A]$ matrices relates simply to the two wave numbers m_x and m_y by:

$$m = (m_x^2 + m_y^2)^{1/2}. \tag{25}$$

Other coordinate systems could be used, the most common one being the polar coordinates. However, from a practical point of view, numerical computations of temperature and/or heat flux distributions according to the scheme explained above are better performed using 2D FFT routines in x and y.

By way of example, Fig. 5 shows the temperature map at the top of the substrate of Fig. 2, so obtained for the geometrical arrangement of heat sources shown in Fig. 4. This corresponds to the special case

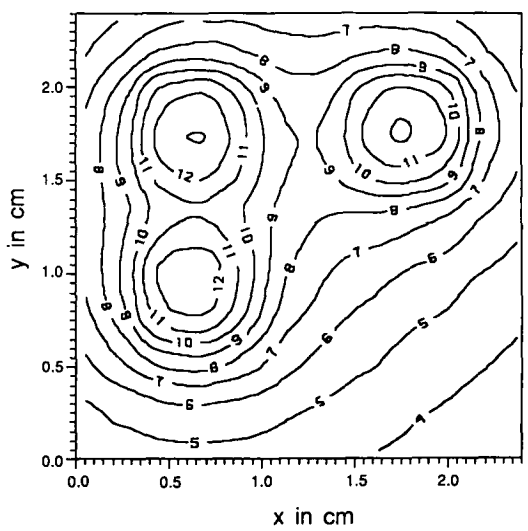

FIG. 5. Thermal map (temperature rise in K) for a 10 W per chip power dissipation (substrate of infinite lateral extent).

of a power MOS multichip module. A 10 W power dissipation is assumed for each MOS transistor.

(c) Multilayered medium of finite extent; parallelepipedic case.

Finite transforms must be employed. For rectangular shaped lateral boundaries (parallelepipedic system), the double finite cosine transform applies for adiabatic boundaries with the pair of relations

$$F(n_x, n_y) = \int_0^L \int_0^l f(x, y) \cos\left(n_x \frac{\pi}{L} x\right) \times \cos\left(n_y \frac{\pi}{l} y\right) dx\, dy \quad (26)$$

$$f(x, y) = \frac{4}{Ll} \sum_{n_x=0}^{\infty} \sum_{n_y=0}^{\infty} \frac{F(n_x, n_y) \cos\left(n_x \frac{\pi}{L} x\right) \cos\left(n_y \frac{\pi}{l} y\right)}{(\delta_{n_x,0}+1)(\delta_{n_y,0}+1)} \quad (27)$$

where L, l are the length and width of the lateral boundary contour and δ is the Kronecker symbol.

Similarly, the double finite sine transform holds for isothermal boundary conditions

$$F(n_x, n_y) = \int_0^L \int_0^l f(x, y) \sin\left(n_x \frac{\pi}{L} x\right) \times \sin\left(n_y \frac{\pi}{l} y\right) dx\, dy \quad (28)$$

$$f(x, y) = \frac{4}{Ll} \sum_{n_x=1}^{\infty} \sum_{n_y=1}^{\infty} F(n_x, n_y) \times \sin\left(n_x \frac{\pi}{L} x\right) \sin\left(n_y \frac{\pi}{l} y\right). \quad (29)$$

Mixed finite cosine–sine transforms are used when a couple of opposite sides are adiabatic and the other is isothermal. If the conditions differ on two opposite sides, the image method can be used taking into account the consequential symmetries in order to convert the temperature and flux distributions into odd or even functions with respect to the x, y coordinates.

In all cases, the m variable of the $[A]$ matrices relates simply to the integers n_x and n_y by:

$$m = \pi \left(\frac{n_x^2}{L^2} + \frac{n_y^2}{l^2}\right)^{1/2}. \quad (30)$$

In practical calculations, FFT algorithms may be used for convenience. Figures 6 and 7 give, as examples, the modified temperature maps for the problem defined in Figs. 2 and 4 as the substrate is delimited as shown by the dashed line contour ABCD. Figure 6 refers to adiabatic lateral boundary conditions and Fig. 7 to mixed conditions (adiabatic AB, BC, DA, isothermal DC).

The parallelepipedic case of multilayered media with a laterally finite extent is not restrictive, though most important in practice. Two-dimensional Fourier representations can be obtained in coordinate systems other than the Cartesian one. These may be suited in the case of cylindrically shaped devices. Of particular interest are circular cylinders with adiabatic or isothermal lateral boundary conditions to which double Fourier–Bessel series apply [15]. However, calculations are much more cumbersome.

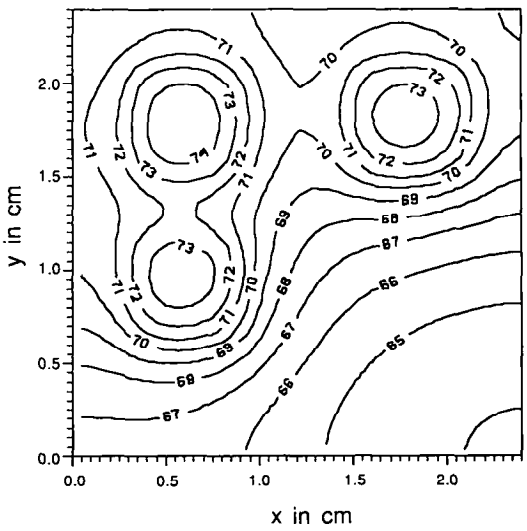

FIG. 6. Thermal map (adiabatic lateral boundary conditions).

4.2. *Unsteady heat flow*

Subject to the use of an additional FFT in time, the calculation procedure, according to equation (16) is the same. Note simply that in $[A]$ matrices, the variable m is now replaced by $m^* = (m^2 + s/D_i)^{1/2}$. With respect to the spatial conditions previously considered

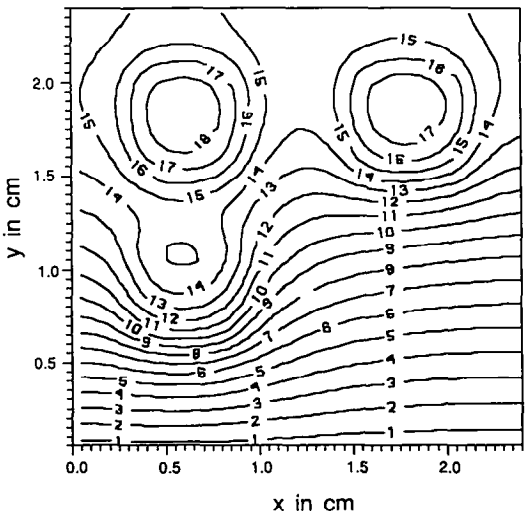

FIG. 7. Thermal map (one isothermal side).

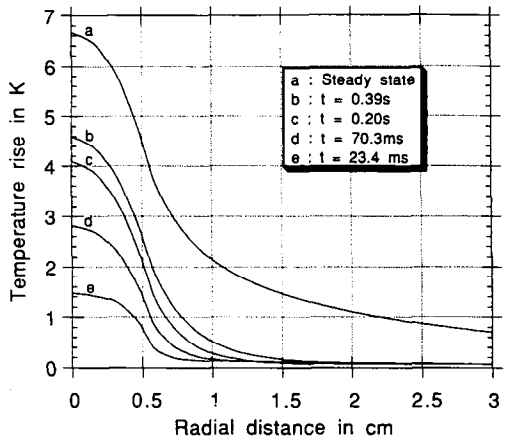

FIG. 8. Evolution in time of radial temperature distribution in case (a) (axisymmetry). Source radius $a = 0.5$ cm, dissipated power $P = 10$ W.

in case (a) (axisymmetry), Fig. 8 displays the evolution in time of the radial temperature distribution at the top surface of the substrate of Fig. 2, for a source radius $a = 0.5$ cm and a dissipated power $P = 10$ W.

4.3. *Alternative calculation procedure*

An alternative computation scheme exists for the examples given. One may restrict the use of the basic relationships equation (16) in the spectral domain to an axisymmetric heat flow due to an elemental source, assuming a lateral indefinite extent of the multilayered medium (case (a)) as defined in Section 4.1. Then, the effective calculation of temperature and/or flux distributions can be done using:

(i) the superposition principle for the influences of a distribution of elemental sources, and

(ii) the method of images to represent the lateral boundary conditions.

The principle of this approach has been published elsewhere [6, 16]. Worthy of note here is the key expression applying to the aforementioned examples. Refering to Fig. 9, it follows from the linearity of the system, that the temperature rise at the top of the substrate considered is given by

$$\theta(x, y) = \int_S c(\rho) p(x', y') \, dx' \, dy'. \qquad (31)$$

$p(x', y')$ denotes the heat flux density at point $P(x', y')$ and $c(\rho) \, dx' \, dy'$ represents the contribution of an element $ds = dx' \, dy'$ of the dissipating area S to the temperature rise at $M(x, y)$. The $c(\rho)$ function which only depends on the radial distance ρ between the two points P and M is therefore the Green's function of the laterally unlimited problem, for the particular value z_1 of the z-coordinate corresponding to the top surface. It can easily be shown, by using the Hankel transform of equation (31) for a unit power point source (axisymmetry, polar coordinates) and by comparing the result with equation (19), that $c(\rho)$ is the inverse transform of $H_{11}(m)/2\pi$

$$\left(\text{or} \quad \frac{A_{12}(m)}{2\pi A_{22}(m)} \right),$$

that is

$$c(\rho) = \frac{1}{2\pi} \int_0^{\infty} m H_{11}(m) J_0(m\rho) \, d\rho. \qquad (32)$$

This function can be computed once and for all for a given multilayered system, thus providing an easy means of temperature mapping through the integral equation (31). If the substrate is laterally shaped as parallelepipedic, the integral must be extended not only to the 'true' dissipating area but also to its images in the adiabatic or isothermal planes that define the system laterally. Figure 10 illustrates the application of the method of images to lateral adiabatic faces. In practice, the influence of images in the far distance can be neglected as the $c(\rho)$ function decreases as ρ increases. Of course, the results obtained in the examples given in Figs. 5–8 are virtually identical. This method may or may not compare favourably with the spectral method previously described, as the case may be, and according to the resolution and accuracy

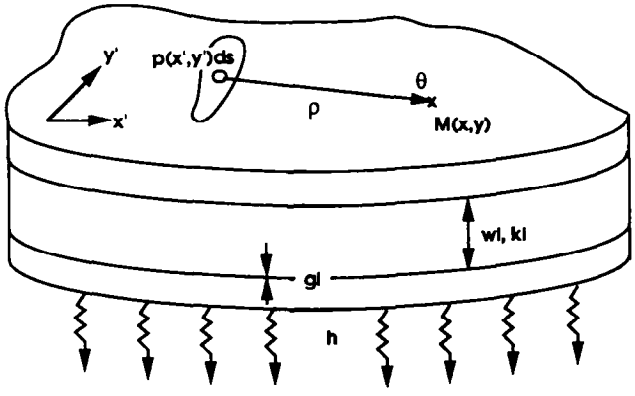

FIG. 9. Introducing schematically the superposition method.

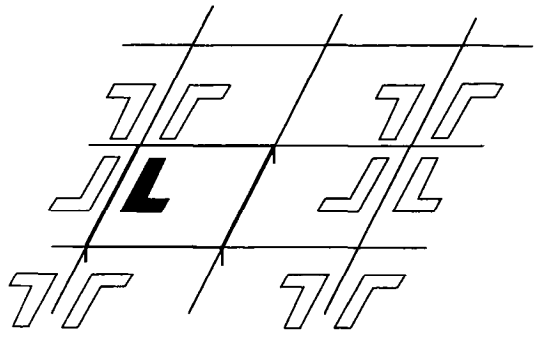

FIG. 10. Illustrating the use of image sources (adiabatic boundary conditions).

required in the calculation. Here, the superposition method is found to need less computational time in the example of Fig. 5 (no lateral constriction of heat flux), but it is less efficient in the example of Fig. 6, due to the large number of images to be taken into consideration. In all cases, memory occupancy and computational time are compatible with the use of PC's (some tenths of seconds with a 0.3 Mflops computer).

5. FURTHER IMPLICATIONS

The parameters of the aforementioned matrices which relate to a layer or a block of layers act as transfer functions fully characterizing the thermal behaviour of the substrate. Thus, the $H_{11}(m)$ parameter defined by equation (20)

$$H_{11}(m) = \left.\frac{\Theta_1(m)}{\Phi_1(m)}\right|_{\Theta_2=0} \tag{33}$$

represents the thermal 'input m-impedance' of the stack when the lower face is forced to remain isothermal. For the composite substrate and radiator shown in Fig. 2, the $H_{11}(m)$ variations describing the overall thermal behaviour of the assembly are plotted in Fig. 11. When comparing to the hybrid parameters

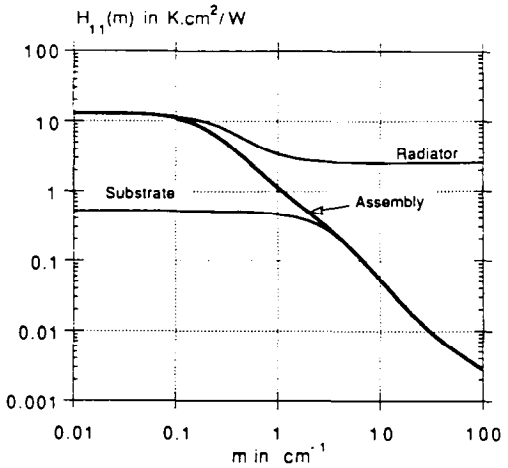

FIG. 11. Illustrating thermal analysis using the $H_{11}(m)$ parameter.

of the substrate and the aluminium cooler considered separately, it appears that at low 'spatial frequencies' (small values of the wave number m) the thermal behaviour is mainly imposed by the cooler, including the interfacial layer of thermal grease, whereas the behaviour of the hybrid substrate prevails at high 'spatial frequencies' (high values of m).

Variations of $H_{11}(m)$ as shown in Fig. 11 are very similar to Bode plots for low-pass filters and can be interpreted in the following manner:

(i) The low 'frequency' asymptote accounts for the 1D thermal resistance (per unit area) of the considered assembly.

(ii) At high 'spatial frequencies' the thermal behaviour of the assembly tends asymptotically toward the response of a semi-infinite medium having the same thermal conductivity as the first layer or toward the interface contact resistance if it exists.

(iii) At intermediate frequency values, cut-off frequencies related to the 3D conductive heat transfer properties of the assembly occur. The inverses of the cut-off frequencies are representative of the heat-source size for which these 3D conductive properties apply.

Thus, these diagrams provide a synthetical overview of the thermal properties of an assembly and in all respects are similar to the Bode plots used for the frequential characterization of electronic circuits.

Other matrix parameters may be used to describe the thermal behaviour of a multilayered thermal system, depending on the kind of homogeneous boundary conditions intended for temperature or flux distributions.

The experimental characterization of multilayered assemblies can be achieved on the basis of the two-port network theory. Taking into account the reciprocity property linked to passivity, the measurement of a consistent set of only three parameters is required. However, the possible procedures indicated by the definition of the various parameters are restricted by practical considerations. Of course, it is easier to measure temperature rises than thermal fluxes and to set adiabatic rather than isothermal boundary conditions, therefore the Z (impedance matrix) parameters are the most easily accessible. These parameters are defined as follows:

$$Z_{11} = \left.\frac{\Theta_1}{\Phi_1}\right|_{\Phi_2=0}$$

$$Z_{12} = -Z_{21} = \left.\frac{\Theta_1}{\Phi_2}\right|_{\Phi_1=0} = -\left.\frac{\Theta_2}{\Phi_1}\right|_{\Phi_2=0}$$

$$Z_{22} = \left.\frac{\Theta_2}{\Phi_2}\right|_{\Phi_1=0}. \tag{34}$$

For simplicity, an axisymmetrical experimental set allows us to use the 0-order Hankel transform (cf. Section 4.1) to handle experimental data (see Fig. 12).

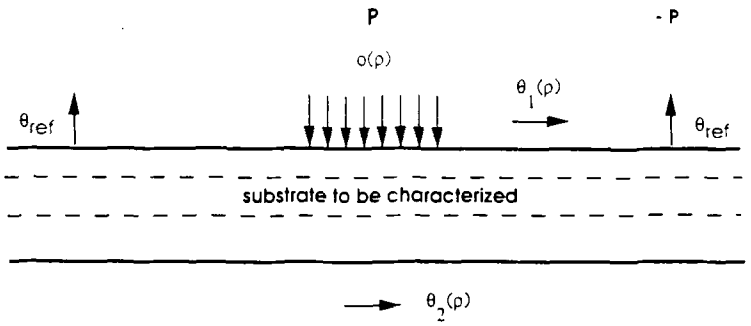

FIG. 12. Schematic of an experimental setting for Z-matrix parameter measurements.

The size of the heat source must be suited to the m-spectral range which should be explored. The injected power must be sinked by a circular heat-sink which is concentric with the heat-source. The radial flux distribution considered for computation must include the injected and removed heat fluxes. Except for the injecting and sinking areas, the substrate has to remain adiabatic everywhere; particular care must therefore be taken to minimize power losses due to convective or radiative heat exchange with the ambient medium.

To illustrate this, Fig. 13 shows a thermogram of a substrate intended for hybrid integrated power circuits. The heat source is a transistor fixed on the substrate in a corner to make optimal use of the symmetry, a circular heat-sinking is provided at some distance. The isothermal lines are quite circular as previously assumed. Temperature distributions $\theta_1(\rho)$ (on the upper face) and $\theta_2(\rho)$ (on the lower face) are measured by I.R. thermography, the Z_{11} and Z_{21} are obtained by dividing the numerical Hankel transform of $\theta_1(\rho)$ and $\theta_2(\rho)$ by the Hankel transform of the heat flux distribution. Turning the substrate upside down, one gets the Z_{12} and Z_{22} parameters in the same way [14]. Details about the experimental setting and data processing will be further discussed in a subsequent publication [17].

6. CONCLUSION

This paper has addressed the fairly old issue of conductive heat transfer through multilayered media. It has been shown that, within integral transform methods, 3D heat flow may be simply described in the

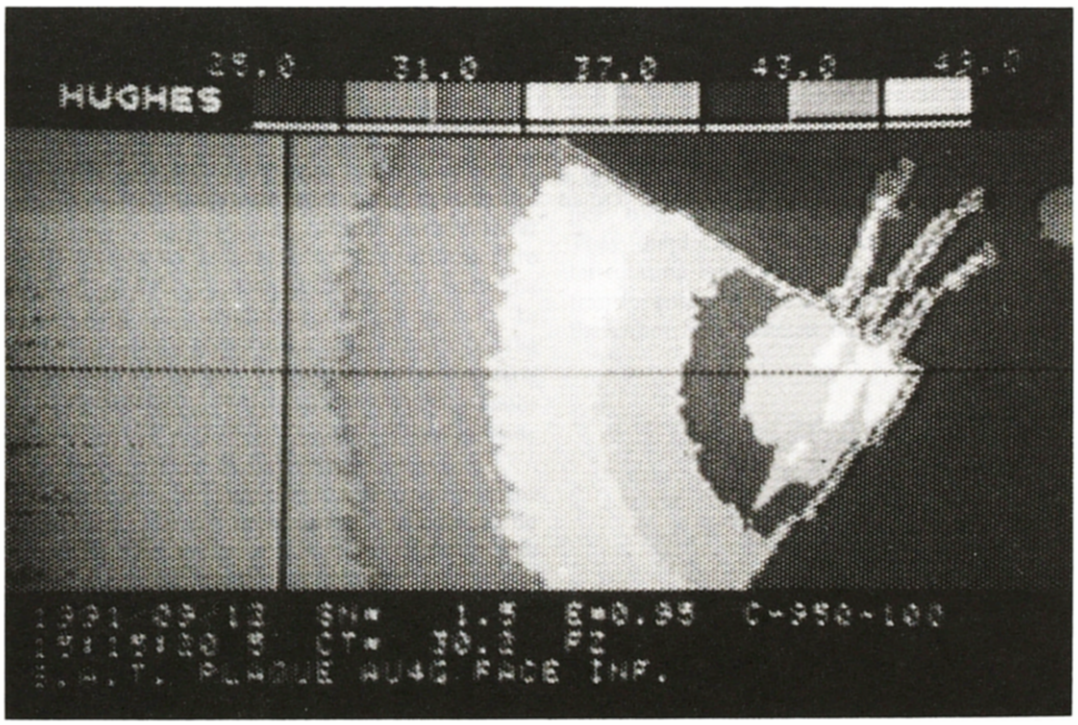

FIG. 13. I.R. thermogram of $\theta_1(\rho)$ distribution illustrating the measurement procedure for a special kind of a power hybrid substrate.

spectral domain using a two-port network formalism similar to that of the linear circuit theory. Each layer or each group of layers, or the whole medium itself can be characterized by a simple chain (or transmission) matrix. This allows the analogy between heat conduction through multilayered media and signal transmission through a cascade of four-terminal networks to be extended to a class of 3D problems.

The concerned class of problems is that in which the stated lateral boundary conditions allow the heat conduction equation to be reduced to an ordinary differential of the form $d^2\Theta/dz^2 = m^2\Theta$, using the available finite or infinite transformations. It involves various cases of interest to engineers (multilayered rectangular parallelepiped for instance), some of which are thoroughly presented as examples. Two different approaches are tested for the practical calculations of temperature and heat flux distributions in the systems considered. These are:

(i) A purely spectral method which uses 2D fast-Fourier transforms.

(ii) A procedure taking advantage of the superposition principle and the method of images.

The former is found to be more efficient in cases where the heat flux is severely constricted by the lateral boundaries of the medium, while the latter is more practical for a widely spread heat flow.

In addition, it is shown that the proposed formalism is well suited to thermal analysis and characterization of multilayered devices.

Acknowledgement—The authors thank Professor A. Degiovanni, from Institut Polytechnique de Lorraine, for informative comments related to this work.

REFERENCES

1. H. S. Carslaw and J. C. Jaeger, *Conduction of Heat in Solids* (2nd Edn). Oxford University Press, Oxford (1959).
2. M. N. Özisik, *Heat Conduction*. John Wiley and Sons, New York (1980).
3. E. Durand, *Electrostatique et Magnétostatique*. Masson et Cie, Paris (1953).
4. A. G. Kokkas, Thermal analysis of multiple layer structures, *IEEE Trans. Electron Devices* **ED-21,** 674–681 (1974).
5. P. Antognetti, G. R. Bisio, F. Curatelli and S. Palara, Three-dimensional transient thermal simulation: application to delayed short circuit protection in power IC's, *IEEE J. Solid State Circuits* **SC-15,** 277–281 (1980).
6. Ph. Leturcq, J. M. Dorkel, A Napieralski and E. Lachiver, A new approach to thermal analysis of power devices, *IEEE Trans. Electron Devices* **ED-34,** 1147–1156 (1987).
7. K. J. Scott, Electrostatic potential Green's functions for multilayered dielectric media, *Philips J. Res.* **45,** 293–324 (1990).
8. P. Brook and J. G. Smith, Spreading resistance of multilayer cylindrical structures, *Electronics Lett.* **9,** 253–254 (1973).
9. T. Harett, Comments on "An analysis of the thermal response of power chip packages", *IEEE Trans. Electron Devices* **ED-33,** 871 (correspondence), (1986).
10. J. Gosse, Sur la conduction thermique variable dans un mur composite à propriétés constantes, *C. R. Acad. Sci. Paris* **t.286,** Série B, 303–306 (1978).
11. P. Duhamel and J. Gosse, Analyse thermique d'un mur composite soumis sur une face à une variation en créneaux de la température, *Int. J. Heat Mass Transfer* **23,** 1663–1671 (1980).
12. A. Degiovanni, Conduction dans un mur multicouche avec sources: extension de la notion de quadripôle, *Int. J. Heat Mass Transfer* **31,** 553–557 (1988).
13. I. N. Sneddon, *Fourier transforms*. McGraw-Hill, New York (1951).
14. Ph. Leturcq, F. E. Ratolojanahary and P. Morillon, Méthodologie de caractérisation thermique de supports et substrats pour l'électronique de puissance, Proceedings of the Colloque Bilan des Actions de Recherche du M.R.T. "Génie Electrique 91", Paris, France, 5–6 Nov. 1991, 83–96.
15. G. N. Watson, *A Treatise on the Theory of Bessel Functions* (2nd Edn). Cambridge University Press (1966).
16. J. M. Dorkel, A. Napieralski and Ph. Leturcq, Implementation of a new method for thermal analysis of plane multilalyered systems, *Numer. Heat Transfer* **13,** 319–336 (1988).
17. F. E. Ratolojahanary, Thèse de Doctorat de l'Institut National des Sciences Appliquées de Toulouse, to be published, July 1993.